Organic LETTERS

Letter

pubs.acs.org/OrgLett

Supramolecular Assembly of Coronene Derivatives for Drug Delivery

Jie Yu,[†] Yong Chen,[†] Yu-Hui Zhang,[†] Xun Xu,[†] and Yu Liu*[,†,‡]

[†]Department of Chemistry, State Key Laboratory of Elemento-Organic Chemistry, Nankai University, Tianjin 300071, P. R. China

[‡]Collaborative Innovation Center of Chemical Science and Engineering (Tianjin), Nankai University, Tianjin 300071, P. R. China

Supporting Information

ABSTRACT: Possessing a small size and C_3-symmetrical rigid backbone, a coronene derivative was synthesized from β-cyclodextrins and hexa-cata-hexabenzocoronene, and then a water-soluble and biocompatible nanographene/polysaccharide supramolecular assembly was successfully fabricated through noncovalent interactions between adamantly grafted hyaluronic acids and β-cyclodextrin-modified hexa-cata-hexabenzocoronene. Moreover, the ternary supramolecular assembly showed not only a fluorescence imaging ability toward cancer cells but also good anticancer activity and low toxicity.

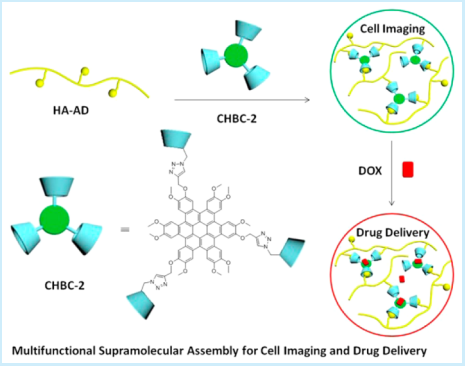

Multifunctional Supramolecular Assembly for Cell Imaging and Drug Delivery

As a kind of fascinating nanomaterial, coronene, also called nanographene, has attracted increasing attention in many fields for use in electronic devices,[1] chemical sensing,[2] and cellular imaging.[3] Given these special characteristics, one can hypothesize that incorporating nanographene into composite materials may bring a breakthrough in nanoscience and technology. In the early stages, scientists mainly focused their efforts on applications of nanographene (such as hexa-peri-hexabenzocoronene) in electronics owing to the special intrinsic properties such as hole-transport capability, charge-carrier mobilities, and π-stacking induced self-assembly abilities.[4] Recently, more attention has been paid to applications of hexa-peri-hexabenzocoronene in biological systems, which displayed an efficacious ability compared to those of graphenes and carbon nanotubes as cell-imaging agents and drug carriers. Prasad et al.[5] prepared a kind of water-dispersible polymeric micelle encapsulated with hexa-peri-hexabenzocoronene nanographene for cellular imaging. Müllen et al.[6] reported the assembly of peptides and hexa-peri-hexabenzocoronene modified with special functional groups for bioprobing. Xiong et al.[7] demonstrated that HepG2 cancer cells could be selectively killed by three-dimensional nanographene. In sharp contrast with hexa-peri-hexabenzocoronene, the application of hexa-cata-hexabenzocoronene in biological areas has been rarely reported. On the other hand, cyclodextrin (CD), a class of cyclic oligosaccharides that can encapsulate various organic or biological molecules in their hydrophobic cavities, and hyaluronic acid (HA), a widely distributed glycosaminogly that can recognize the CD44/RHAMM receptors overexpressed on cancer cells,[8] are water-soluble, biocompatible, and widely used in biological systems as drug carriers.[9] In this work, we report a nanographene/polysaccharide supramolecular assembly, i.e., **CHBC-2/HA-AD** assembly (Scheme 1), constructed from hexa-cata-hexabenzocoronene,[10]

Scheme 1. Construction of DOX@CHBC-2/HA-AD Supramolecular Assembly

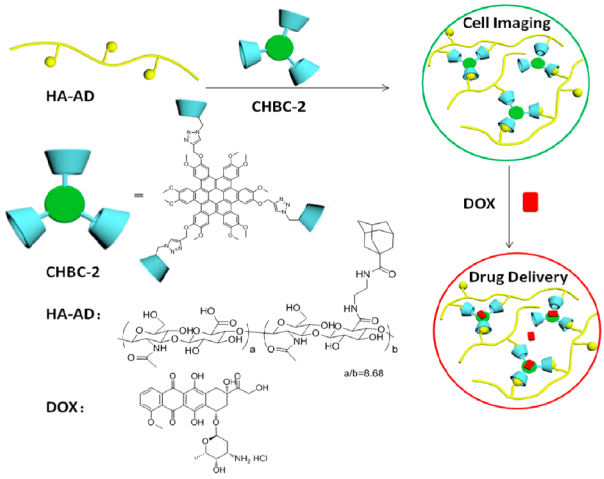

β-CD, and HA via a bottom-up strategy. First, **CHBC-2**, which possesses three β-CD cavities and a C_3-symmetrical rigid fluorescent nanographene core, was synthesized in satisfactory yield (52%) through a click reaction. Subsequently, the targeted polysaccharide HA was noncovalently linked to **CHBC-2** through the strong binding of adamantanyl moieties grafted to HA with β-CD cavities.[11]

There are several advantages to combining nanographene with β-CD and HA: (1) it is possible to take advantage of the intrinsic fluorescence properties of coronene derivatives (such

Received: July 25, 2016
Published: September 2, 2016

DOI: 10.1021/acs.orglett.6b02183
Org. Lett. 2016, 18, 4542–4545

as anti-photobleaching ability,[3] strong fluorescence emission, and excitability at the β/p band in the UV/vis region), the C_3-symmetrical nanographene could act as a fluorescence probe in cell imaging reagents; (2) the introduction of β-CD and HA units can not only efficiently increase the water solubility and biocompatibility of nanographene but also prevent the self-quenching of graphene, leading to fluorescence emission that could be readily distinguished by the naked eye; (3) encapsulation and loading efficiency of anticancer drugs could be improved by introducing the small and rigid backbone nanographene to this drug delivery system. Furthermore, the noncovalently loaded anticancer drugs could be readily delivered to cancer cells owing to the targeting ability deriving from the hyaluronated adamantane (**HA-AD**) chains, in which the HA skeleton can specifically recognize HA receptor-overexpressing tumor cells in cancer metastasis. Consequently, the **CHBC-2**/**HA-AD** assembly could not only act as an imaging agent with photostability and low toxicity toward cancer cells but also be utilized as a convenient platform for targeted drug delivery. To the best of our knowledge, this kind of nanographene/polysaccharide supramolecular conjugate has not been reported so far despite the advantages mentioned here.

Synthetic route to the water-soluble C_3-symmetrical nanographene derivative **CHBC-2** is shown in Scheme 2. Vanillin

Scheme 2. Synthetic Route to CHBC-2

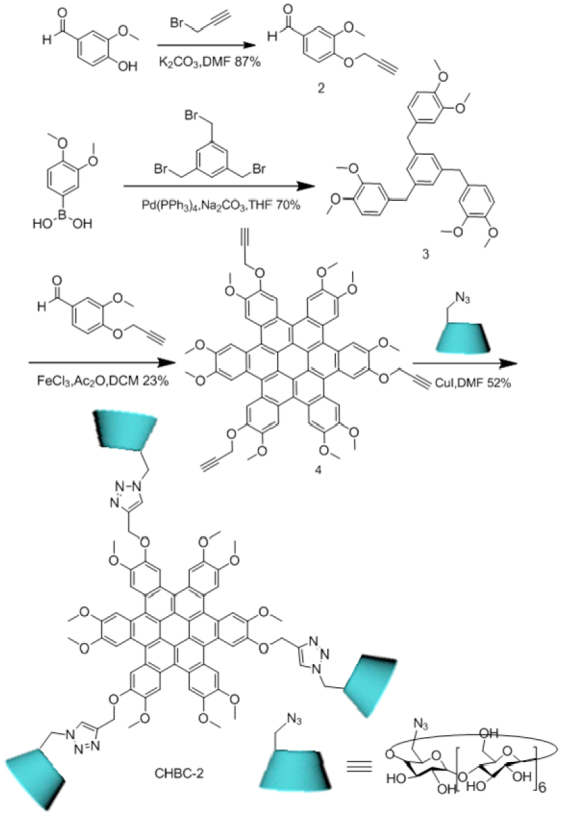

reacted with 3-bromopropyne in the presence of K_2CO_3 to give compound **2**. Intermediate compound **3** was synthesized by Suzuki reaction of 3,4-dialkoxyphenylboronic acid with 1,3,5-tri(bromomethyl)benzene. Although a series of C_3-symmetrical hexa-cata-hexabenzocoronene derivatives were successfully synthesized, further derivation is still difficult. According to the reported method of Wei et al.,[10] the intermediate compound **3** reacted with compound **2** in the presence of $FeCl_3$ and anhydrous acetic anhydride in anhydrous DCM to give the building block with three alkynyl-substituted hexa-cata-hexabenzocoronenes **4** in 23% yield. Subsequently, three β-CD-modified nanographene has been synthesized from **4** and excess 6-deoxy-6-azido-β-CD in anhydrous DMF by means of "click chemistry" in 52% yield. As shown in Figure S1, two singlet signals lying at 5.06 and 2.63 ppm were assigned to the protons of methylene and alkynyl in compound **4**, respectively. A clear single peak at 8.29 ppm was assigned to the proton of the triazole ring (Figure S4), indicating that three β-CDs were grafted to the nanographene. Moreover, both compound **4** and **CHBC-2** were further confirmed by MALDI-TOF experiments (Figures S3 and S6).

Subsequently, the **CHBC-2**/**HA-AD** assembly could be constructed conveniently by the association of **CHBC-2** with **HA-AD** in aqueous solution due to the strong binding of adamantane moieties to the β-CD cavity in **CHBC-2**.[11] By monitoring the UV−vis spectrum of **CHBC-2**/**HA-AD** at 470 nm, the photometric standard curve of **CHBC-2**/**HA-AD** was measured (Figures S22 and S23). The solution of CHBC-2/HA-AD at 500 μM was turbid; thus, the solution was centrifuged and filtrated. The UV−vis spectrum of the obtained clear solution was recorded, and the water solubility of supramolecular assembly was calculated as 6.98 mg/mL. The obvious Tyndall effect (Figure S15) indicated the formation of a large CHBC-2/HA-AD supramolecular assembly. Both TEM and SEM images at different magnifications (Figure 1 and

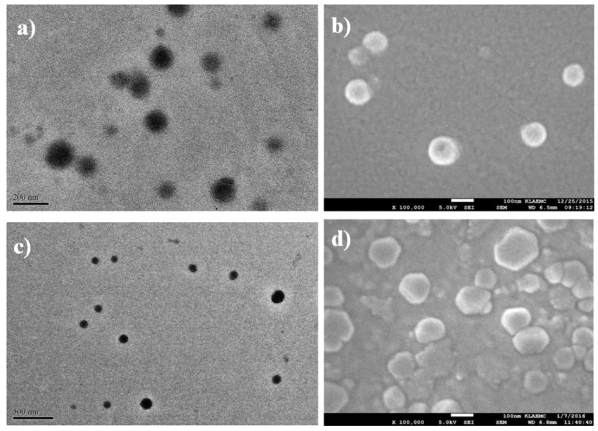

Figure 1. TEM (a, c) and SEM (b, d) images of **CHBC-2**/**HA-AD** (a, b) and **DOX@CHBC-2**/**HA-AD** (c, d).

Figure S17) showed that the **CHBC-2**/**HA-AD** assembly existed as discrete spherical particles with an average diameter of ca.140 nm, accompanied by a relatively narrow particle size distribution (Figure S17i). In addition, the hydrodynamic diameter of the assembly was also measured by DLS to be ca. 234 nm. Moreover, the effect of the **HA-AD**/**CHBC-2** ratio on the structure of supramolecular assemblies was also studied. As shown in Figure S24, the sizes of supramolecular assemblies gradually increased and then slowly decreased with increasing **HA-AD**/**CHBC-2** ratio, and a **HA-AD**/**CHBC-2** ratio of 3:1 was the lowest ratio to obtain soluble assembly.

ζ potential measurements gave a ζ potential of **CHBC-2**/**HA-AD** assembly as −45 mV, indicating that the assembly possessed the capability of associating cationic substrates. It is noteworthy that, when excited at the β/p band of hexa-cata-

DOI: 10.1021/acs.orglett.6b02183
Org. Lett. 2016, 18, 4542−4545

hexabenzocoronene, **CHBC-2** emitted bright green fluorescence (Figure S8), which could be readily distinguished by the naked eye. This photophysical property of **CHBC-2** is quite different from that of reported graphenes that barely fluoresced or emitted in at near-infrared fluorescence.[12] Furthermore, when **HA-AD** (0−3.0 equiv) was added to the solution of CHBC-2, the fluorescence intensity of **CHBC-2** did not change (Figure S9). Significantly, the **CHBC-2/HA-AD** assembly also presented good luminescence properties in living cells. Figure 2

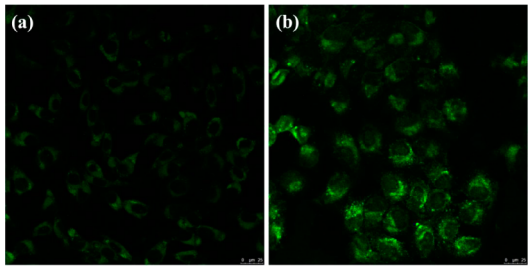

Figure 2. Fluorescence confocal microscopic images of NIH3T3 (a) and MCF-7 cells (b) after 24 h incubation with **CHBC-2/HA-AD**.

shows the fluorescence confocal microscopic images of nonluminescent MCF-7 cancer cells (human breast cancer cell, HA receptor overexpressed) and NIH3T3 cells (mouse embryo fibroblast cell, HA receptor negative) after treatment with the **CHBC-2/HA-AD** assembly. As shown in Figure 2, after 24 h incubation, NIH3T3 cells only presented very weak fluorescence, but nearly all of the MCF-7 cancer cells were luminescent under the fluorescence microscope, indicating a quite high imaging property of the **CHBC-2/HA-AD** assembly toward cancer cells. In the control experiments, neither NIH3T3 nor MCF-7 cells fluoresced in the absence of the **CHBC-2/HA-AD** assembly under the same conditions. A possible explanation may be that the high affinity of the HA shell in the **CHBC-2/HA-AD** assembly toward HA receptors on cancer cells facilitated the receptor-mediated endocytosis of **CHBC-2/HA-AD** assembly into cancer cells, but this process was impeded in NIH3T3 cells to a great extent because of the lack of HA receptors. This observation indicated the potential application of the **CHBC-2/HA-AD** assembly as an efficient imaging agent for cancer cells. The drug loading and releasing behaviors of the **CHBC-2/HA-AD** assembly were investigated by UV−vis, fluorescence, and ζ-potential experiments with doxorubicin hydrochloride (**DOX**) as a model substrate. As shown in Figure S13, the UV−vis spectrum of **DOX@CHBC-2/HA-AD** showed two shoulders (334 and 425 nm), a maximum (390 nm) assigned to the characteristic absorption of **CHBC-2/HA-AD** assembly, and a maximum at 490 nm assigned to the characteristic absorption of **DOX**. With the gradual addition of **DOX** (0−3.0 equiv), the fluorescence intensity of **CHBC-2/HA-AD** assembly gradually decreased. The fluorescence-quenching efficiency was calculated to be 93.1% (Figure S10). In addition, a new fluorescence peak assigned to the emission of **DOX** appeared at 592 nm and gradually increased. A possible reason may be the photoinduced electron transfer process and/or the Förster resonance energy transfer process between **CHBC-2** and **DOX**. Moreover, the ζ-potential of the **DOX@CHBC-2/HA-AD** assembly was measured to be −33 mV, much higher than that of the **CHBC-2/HA-AD** assembly alone (−45 mV), which was ascribed to the loading of positively charged **DOX**.

It is also noteworthy that, even after the loading of **DOX**, the **CHBC-2/HA-AD** assembly still maintained a negative surface charge, which would favor its biocompatibility and prolong its circulation time in vivo. These results jointly indicate that the anticancer drug **DOX** was efficiently loaded onto the **CHBC-2/HA-AD** assembly to form biocompatible **DOX@CHBC-2/HA-AD** conjugates. By monitoring the UV−vis spectrum of **DOX** at 490 nm, the photometric standard curve of **DOX** was recorded (see Figures S11 and S12). Accordingly, the encapsulation and loading efficiency of **DOX** were calculated to be 81.4% and 11.7%, respectively (Figure S13), which was much higher than the previously reported drug delivery system.[9c] In this assembly, the rigid backbone nanographene played an important role in enhancing the encapsulation and loading efficiency. TEM and SEM images at different magnifications (Figure 1 and Figure S17) showed that, after **DOX** loading, the **CHBC-2/HA-AD** assembly remained its original morphology, accompanied by a relatively narrow particle size distribution (Figure S17j) but its average diameter contracted to ca. 90 nm (hydrodynamic diameter contracted to ca. 221 nm measured by DLS), and this size would facilitate the endocytosis of **DOX@CHBC-2/HA-AD** into cancer cells.[13] On the other hand, the release behavior of **DOX@CHBC-2/HA-AD** was also examined in physiological environments (0.01 M phosphate buffer solution, pH = 5.7 or 7.2, 37 °C). The **DOX@CHBC-2/HA-AD** displayed the slow and controlled release of drug in either an acidic or a neutral environment (Figure S14), and the release efficiency of **DOX** from **DOX@CHBC-2/HA-AD** at pH 5.7 (the endosomal pH of a cancer cell) was 1.4 times higher than that at pH 7.2 (physiological pH). This pH-responsive release of drug in the cancer cell environment will not only improve its cytotoxic efficacy against tumor cells but also reduce the toxicity of drug to normal tissues.

It is also important to examine the in vitro cytotoxicity of **DOX@CHBC-2/HA-AD**. As shown in Figure S19, after a 24 h incubation, **DOX@CHBC-2/HA-AD** displayed a higher anticancer activity (relative cellular viability 42.0%) than free **DOX** (relative cellular viability 57.3%) toward MCF-7 cancer cells. The half-maximal inhibitory concentration (IC_{50}) of **DOX@CHBC-2/HA-AD** was calculated to be 1.1 μg/mL (Figure S21). This result was 60 times lower than the corresponding value of our previously drug delivery assembly.[14] A possible reason may be that the specific association between HA units in **DOX@CHBC-2/HA-AD** and HA receptors on cancer cell surfaces facilitated the incorporation and uptake of **DOX@CHBC-2/HA-AD** into MCF-7 cancer cells through the receptor-mediated endocytosis. Furthermore, when an excess amount of HA was added, the relative cellular viability of MCF-7 increased to 47.0% after treatment with **DOX@CHBC-2/HA-AD**, attributed to the fact that that HA receptors on MCF-7 cell surfaces were blocked by an excess amount of HA.[9c] In addition, **DOX@CHBC-2/HA-AD** gave a higher cellular viability (79.4%) toward the NIH3T3 cells than free **DOX** (71.6%) after 24 h, indicating the low toxicity of **DOX@CHBC-2/HA-AD** toward normal cells. In control experiments, the **CHBC-2/HA-AD** assembly displayed nearly no cytotoxicity toward both MCF-7 and NIH3T3 cells. These phenomena jointly indicated that the **CHBC-2/HA-AD** supramolecular assembly could be utilized as a safe and promising targeted drug delivery platform. Similar results were also observed in the case of 48 h of incubation.

DOI: 10.1021/acs.orglett.6b02183
Org. Lett. 2016, 18, 4542−4545

In summary, a water-soluble C_3-symmetrical rigid backbone nanographene, which has application potential as a cell imaging agent, was successfully synthesized and characterized by NMR, MALDI-TOF MS, UV/vis, and fluorescence. Subsequently, a multifunctional supramolecular platform was successfully constructed by the supramolecular assembly of β-CD-modified hexa-cata-hexabenzocoronene with the adamantyl-grafted HA. As two typical examples of possible applications, it could selectively image cancer cells over normal cells, and its conjugate with the anticancer drug **DOX** displayed a higher antitumor activity and a lower toxicity than the free **DOX**. Considering the good water solubility and biocompatibility of both β-CD-modified hexa-cata-hexabenzocoronene and adamantyl-grafted HA, this achievement would not only provide new access to associating nanographene with functional substrates but also extend the possible application of nanographene in many fields of pharmaceutical chemistry and biological technology.

■ ASSOCIATED CONTENT

Supporting Information

The Supporting Information is available free of charge on the ACS Publications website at DOI: 10.1021/acs.orglett.6b02183.

Experimental details (PDF)

■ AUTHOR INFORMATION

Corresponding Author

*E-mail: yuliu@nankai.edu.cn.

Notes

The authors declare no competing financial interest.

■ ACKNOWLEDGMENTS

We thank the NNSFC (21432004, 21272125, and 91527301) for financial support.

■ REFERENCES

(1) (a) Hill, J. P.; Jin, W. S.; Kosaka, A.; Fukushima, T.; Ichihara, H.; Shimomura, T.; Ito, K.; Hashizume, T.; Ishii, N.; Aida, T. *Science* **2004**, *304*, 1481−1483. (b) Cao, J.; Liu, Y.-M.; Jing, X.; Yin, J.; Li, J.; Xu, B.; Tan, Y.-Z.; Zheng, N. *J. Am. Chem. Soc.* **2015**, *137*, 10914−10917.

(2) (a) Vij, V.; Bhalla, V.; Kumar, M. *ACS Appl. Mater. Interfaces* **2013**, *5*, 5373−5380. (b) Zhu, P.-C.; Luo, L.-N.; Cen, P.-Q.; Li, J.-T.; Zhang, C. *Tetrahedron Lett.* **2014**, *55*, 6277−6280.

(3) Zhang, C.; Liu, Y.; Xiong, X.-Q.; Peng, L.-H.; Gan, L.; Chen, C.-F.; Xu, H.-B. *Org. Lett.* **2012**, *14*, 5912−5915.

(4) (a) Yamamoto, Y.; Zhang, G.; Jin, W.; Fukushima, T.; Ishii, N.; Saeki, A.; Seki, S.; Tagawa, S.; Minari, T.; Tsukagoshi, K.; Aida, T. *Proc. Natl. Acad. Sci. U. S. A.* **2009**, *106*, 21051−21056. (b) Watson, M. D.; Fechtenkotter, A.; Müllen, K. *Chem. Rev.* **2001**, *101*, 1267−1300. (c) van de Craats, A. M.; Stutzmann, N.; Bunk, O.; Nielsen, M. M.; Watson, M.; Mullen, K.; Chanzy, H. D.; Sirringhaus, H.; Friend, R. H. *Adv. Mater.* **2003**, *15*, 495−499. (d) Yamamoto, Y.; Fukushima, T.; Suna, Y.; Ishii, N.; Saeki, A.; Seki, S.; Tagawa, S.; Taniguchi, M.; Kawai, T.; Aida, T. *Science* **2006**, *314*, 1761−1764.

(5) Zheng, Q.; Ohulchanskyy, T. Y.; Sahoo, Y.; Prasad, P. N. *J. Phys. Chem. C* **2007**, *111*, 16846−16851.

(6) Yin, M.; Shen, J.; Pisula, W.; Liang, M.; Zhi, L.; Müllen, K. *J. Am. Chem. Soc.* **2009**, *131*, 14618−14619.

(7) Xiong, X.; Gan, L.; Liu, Y.; Zhang, C.; Yong, T.; Wang, Z.; Xu, H.; Yang, X. *Nanoscale* **2015**, *7*, 5217−5229.

(8) (a) Luo, Y.; Ziebell, M. R.; Prestwich, G. D. *Biomacromolecules* **2000**, *1*, 208−218. (b) Park, K. M.; Yang, J.-A.; Jung, H.; Yeom, J.; Park, J. S.; Park, K.-H.; Hoffman, A. S.; Hahn, S. K.; Kim, K. *ACS Nano* **2012**, *6*, 2960−2968. (c) Kong, J. H.; Oh, E. J.; Chae, S. Y.; Lee, K. C.; Hahn, S. K. *Biomaterials* **2010**, *31*, 4121−4128.

(9) (a) Bachar, G.; Cohen, K.; Hod, R.; Feinmesser, R.; Mizrachi, A.; Shpitzer, T.; Katz, O.; Peer, D. *Biomaterials* **2011**, *32*, 4840−4848. (b) Rivkin, I.; Cohen, K.; Koffler, J.; Melikhov, D.; Peer, D.; Margalit, R. *Biomaterials* **2010**, *31*, 7106−7114. (c) Zhang, Y. M.; Cao, Y.; Yang, Y.; Chen, J. T.; Liu, Y. *Chem. Commun.* **2014**, *50*, 13066−13069. (d) Yang, Y.; Zhang, Y. M.; Chen, Y.; Chen, J. T.; Liu, Y. *J. Med. Chem.* **2013**, *56*, 9725−9736.

(10) Zhang, Q.; Peng, H.; Zhang, G.; Lu, Q.; Chang, J.; Dong, Y.; Shi, X.; Wei, J. *J. Am. Chem. Soc.* **2014**, *136*, 5057−5064.

(11) Eftink, M. R.; Andy, M. L.; Bystrom, K.; Perlmutter, H. D.; Kristol, D. S. *J. Am. Chem. Soc.* **1989**, *111*, 6765−6772.

(12) (a) Fan, F.-R. F.; Park, S.; Zhu, Y.; Ruoff, R. S.; Bard, A. J. *J. Am. Chem. Soc.* **2009**, *131*, 937−939. (b) Orecchioni, M.; Cabizza, R.; Bianco, A.; Delogu, L. G. *Theranostics* **2015**, *5*, 710−723. (c) Chen, J.-L.; Yan, X.-P. *Chem. Commun.* **2011**, *47*, 3135−3137.

(13) (a) Canton, I.; Battaglia, G. *Chem. Soc. Rev.* **2012**, *41*, 2718−2739. (b) Hillaireau, H.; Couvreur, P. *Cell. Mol. Life Sci.* **2009**, *66*, 2873−2896.

(14) Li, N.; Chen, Y.; Zhang, Y. M.; Yang, Y.; Su, Y.; Chen, J. T.; Liu, Y. *Sci. Rep.* **2014**, *4*, 4164.

DOI: 10.1021/acs.orglett.6b02183
Org. Lett. 2016, 18, 4542−4545